



JGR Atmospheres

RESEARCH ARTICLE

10.1029/2021JD035097

Key Points:

- The maximum halo/sprite production of Matthew inferred from lightning data lags behind the maximum hurricane intensity by one day
- The strong updraft (especially at low levels) provides the favorable condition for the negative halo production above the inner core
- Similar to continental mesoscale convective systems, the outer rainband region of Matthew has been proficient in halo/sprite production

Correspondence to:

J. Yang, yangj@mail.iap.ac.cn

Citation

Huang, A., Yang, J., Cummer, S. A., Lyu, F., & Liu, N. (2021). Examining the capacity of hurricane Matthew (2016) in spawning halo/sprite-producible lightning strokes during its lifetime. *Journal of Geophysical Research: Atmospheres*, 126, e2021JD035097. https://doi.org/10.1029/2021JD035097

Received 16 APR 2021 Accepted 14 JUN 2021

Examining the Capacity of Hurricane Matthew (2016) in Spawning Halo/Sprite-Producible Lightning Strokes During Its Lifetime

Anjing Huang^{1,2,3}, Jing Yang³, Steven A. Cummer¹, Fanchao Lyu⁴, and Ningyu Liu⁵

¹Electrical and Computer Engineering Department, Duke University, Durham, NC, USA, ²University of Chinese Academy of Sciences, Beijing, China, ³Key Laboratory of Middle Atmosphere and Global Environment Observation (LAGEO), Institute of Atmospheric Physics, Chinese Academy of Sciences, Beijing, China, ⁴Nanjing Joint Institute for Atmospheric Sciences, Chinese Academy of Meteorological Sciences, Nanjing, China, ⁵Department of Physics, University of New Hampshire, Durham, NH, USA

Abstract This paper evaluated the overall capability of a hurricane in posing the electromagnetic impact on the high-altitude atmosphere. Oceanic thunderstorms are more efficient in producing negative polarity cloud-to-ground (CG) strokes with large impulse charge moment changes (iCMCs) than continental thunderstorms. As the strongest oceanic thunderstorms, hurricanes' capability to produce transient luminous events is desired to be examined. Here, we investigated the halo/sprite production of hurricane Matthew (2016) by examining the iCMCs of lightning detected by the World-Wide Lightning Location Network hour by hour at nighttime, based on the ultra-low frequency (ULF) magnetic field of the lightning strokes. Matthew was likely an active halo/sprite producer and produced more than 1,000 halo/sprite producible strokes (H/S strokes) with iCMCs exceeding the threshold (200 C km) for producing halo/sprite. The peak of H/S strokes in the outer rainband lags about one day behind the maximum hurricane strength. Additionally, the absence of positive sprite-producible strokes in the inner core (0–100 km) of Matthew may be attributed to the spiral warm cloud feature, although many negative halos could be produced instead because 112 halo/sprite producible strokes were identified here with 89% being negative. In contrast, the outer rainband exhibits some features of the trailing stratiform region of continental mesoscale convective systems (MCSs) and has been a favorable region of halo/ sprite production. Overall, the inner core of Matthew and probably also that of other hurricanes bear the features that make the oceanic thunderstorms a proficient producer of negative halos but not sprites.

Plain Language Summary The ground-based observations in the past three decades indicate that almost all sprites captured over continental thunderstorms are produced by positive cloud-to-ground (CG) lightning. However, the space-born observations from the Imager of Sprites and Upper Atmospheric Lightning (ISUAL) aboard the FORMOSAT-2 satellite indicate a relatively high proportion (~25%) of sprites produced by negative CGs in the ocean, forming a sharp contrast in the generation of sprite-producible negative lightning between continental and oceanic thunderstorms. Interestingly, one amateur photographer captured tens of sprites over hurricane Matthew (2016), but none of these observations were produced by negative strokes. This inconsistency warrants a dedicated study on the halo/sprite production during the entire lifetime of Matthew. A thorough examination of halo/sprite-producible strokes generated by Matthew during its 11-days life cycle indicates that the halo/sprite production of the entire hurricane is divided into two regions: the inner core is favorable for negative halo production, and the outer rainband is a region hosting both positive and negative halo/sprite-producible strokes. Moreover, the outer rainband exhibits a bipolar pattern with positive charges located in the peripheral area. Those observations support the similarities between the outer rainband of Matthew and the trailing stratiform region of continental MCSs.

1. Introduction

Satellite observations indicate that lightning activity exhibits a predominance over land areas with an average land/ocean ratio of approximately 10:1 (Christian et al., 2003), which is also shown by the lightning detection results of ground-based sensor networks (Said et al., 2013). However, both space-born and

© 2021. American Geophysical Union. All Rights Reserved.

HUANG ET AL. 1 of 15



ground-based observations indicate that lightning strokes spawned in oceanic thunderstorms might bear substantially high strength (i.e., with a much larger peak current) than that produced by continental thunderstorms (e.g., Said et al., 2013). These observations suggest lightning in the ocean is more effective in depositing electromagnetic energy into the mesosphere. In particular, as one major class of lightning-induced transient luminous events (TLEs) in the mesosphere (Boccippio et al., 1995; Lyons & Keen, 1994; Sentman et al., 1995), sprites do not show a scarcity over oceanic thunderstorms (A. B. Chen et al., 2008; A. B. -C. Chen et al., 2019).

There is indeed a significant difference between continental and oceanic thunderstorms in the causative lightning of sprites. The ground-based observations, mainly conducted in the continental regions, show that sprites are predominately (more than 99%) produced by positive cloud-to-ground (CG) lightning strokes transferring positive charge from in-cloud reservoirs to ground (Boccippio et al., 1995; Lu et al., 2013; Williams et al., 2007). The observations from space-based platforms, however, indicate that sprites produced by negative CG strokes are more frequently (nearly 20%) observed above oceanic thunderstorms (A. B. -C. Chen et al., 2019; Lu et al., 2017). The enhanced energetics of oceanic thunderstorms in producing dielectric mesospheric breakdown are more prominent for the similar phenomenon known as halos with even shorter duration (typically about 1 ms) in the middle atmosphere (Frey et al., 2007; Lu et al., 2018; Miyasato et al., 2002). As the prompt optical emission that is usually centered at about 80 km altitude (Frey et al., 2007), halos are closely related to the impulsive charge transfer of causative CG strokes, which usually bear insufficient duration for charge transfer to support the development of downward streamers (Li et al., 2012; Qin et al., 2014).

Due to the difficulties of observation, there are only very limited reports of ground-based sprite observations above oceanic thunderstorms. Huang, Lu, Yue et al. (2018) reported the observation of more than 40 sprites over an Atlantic hurricane (Matthew in 2016) while it passed to the north of Venezuela. Nonetheless, all these sprites were produced by positive CG strokes spawned in the outer rainband (>100 km) region, and there was no sprite observation above the inner core (within 100 km or so) region. However, the optical observations within a limited time of this case study are not sufficient to distinguish tropical cyclones (TCs) from typical oceanic thunderstorms that produce the sprite-producing negative CG strokes. Because tropical cyclones are large-scale thunderstorm systems that usually traverse over thousands of kilometers during a typical life cycle of several days, and as they could exhibit varying features at different stages of evolution, it remains necessary to further investigate the sprite genesis of TCs.

In this paper, we conducted a more comprehensive analysis of the capabilities and characteristics of hurricane Matthew (2016) on producing electromagnetic coupling disturbance between the troposphere and lower ionosphere. More specifically, we focused the analysis on the CG strokes that produced sufficiently large impulse charge moment changes (iCMCs) to produce sprites or halos. We scrutinized the connection between halo/sprite production and the intensity of hurricane Matthew, providing an indication for future halo/sprite observations above TCs. In addition, we compared the outer rainband of the hurricane with continental mesoscale convective systems (MCSs) as the well-known sprite-producing meteorological systems to discuss the differences and similarities between these two sprite-producing systems. The main objective of this work is to get more insights into the impact of oceanic thunderstorms on the lower ionosphere.

2. Measurements and Data

As the most devastating TC in 2016, hurricane Matthew developed a 12-days lifetime from September 28 to October 9 (Miller et al., 2018) and it reached the hurricane intensity on September 29. On the early morning of September 30, Matthew underwent the rapid intensification (RI; the increase in the maximum sustained winds of a tropical cyclone over a 24-h period exceeds 30 knots). Figure 1 shows the best track (computed from six-hourly positions and intensities; Stewart, 2016) for hurricane Matthew during its lifespan, and the yellow rectangle represents the period of RI.

2.1. Data for Lightning Analysis

As shown in Figure 2a, after the 24-h period of RI from September 30, Matthew reached the estimated peak intensity of 145 kt (shown as the best track maximum sustained surface wind speed) at 0000 UTC on

HUANG ET AL. 2 of 15

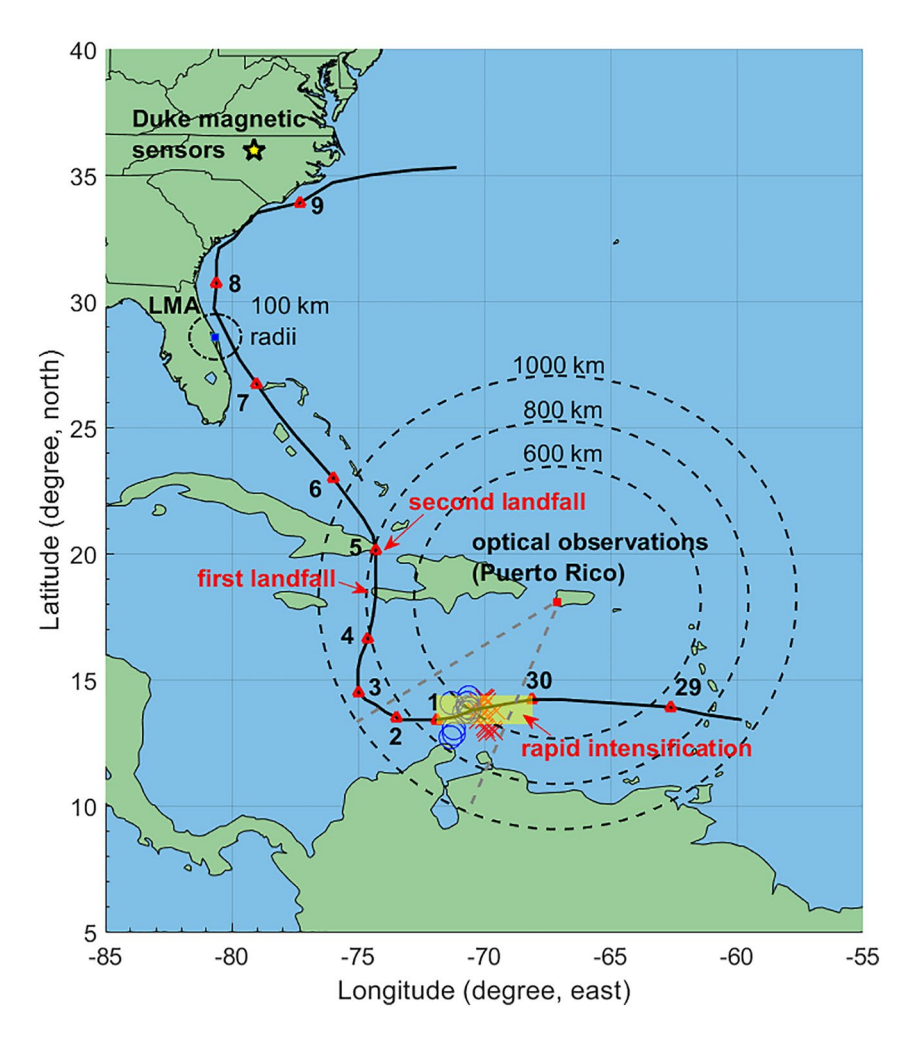


Figure 1. Full development path (from September 29 to October 9) of Hurricane Matthew after it reached the hurricane intensity. The yellow rectangle represents a rapid intensification (RI) from 0000 UTC, September 30 to 0000 UTC, October 1. At 1100 UTC October 4 and 0000 UTC October 5, Matthew made landfall near Anglais, Haiti and near Juaco, Cuba, respectively hurricane. The optical observations of sprites were conducted on the evening of October 1 and October 2 from Puerto Rico (Huang, Lu, Yue et al., 2018). The blue circles and red crosses represent the negative and red sprites detected by the optical observations. Matthew approached the eastern coast of Florida on October 7. We examined the video observation from a low-light-level video imaging system and the data from Lightning Mapping Array (LMA) network when Matthew entered their detection ranges on October 7. But no evidence for sprite production and other supportive information were found above Matthew. The numbers near the hurricane path represent the dates when Matthew arrived at the nearest best track positions plotted as points in the path at 0000 UTC.

October 1. About 40 sprites were captured by camera on October 1 and 2 from Cabo Rojo, Puerto Rico after the RI (Huang, Lu, Zhang et al., 2018), and the parent lightning strokes for some of these sprites detected by the World-Wide Lightning Location Network (WWLLN) were indicated by red crosses and blue circles in Figure 1. The lightning data during Matthew are from WWLLN, which is an experimental lightning detection network with contributions from over 40 universities and institutions worldwide (Lay et al., 2004). For relatively intense lightning strokes, the location accuracy of WWLLN is typically better than 10 km (Abarca et al., 2010; Huang, Lu, Zhang et al., 2018). For the lightning discharges detected by WWLLN, the magnetic signals were recorded with two pairs of induction coils installed in Duke Forest (35.970°N, 79.094°E), whose frequency range is <0.1–400 Hz (referred to as ultra-low frequency, ULF), and 50 Hz to 25 kHz (very-low frequency, VLF), respectively (e.g., Lu et al., 2013).

On October 7, Matthew made landfall on the west shore of Grand Bahama Island, and approached the east coast of Florida. Therefore, we examined the video observation from a low-light-level video imaging system deployed on the campus of Florida Institute of Technology (e.g., Boggs et al., 2016) and the New Smyrna

HUANG ET AL. 3 of 15

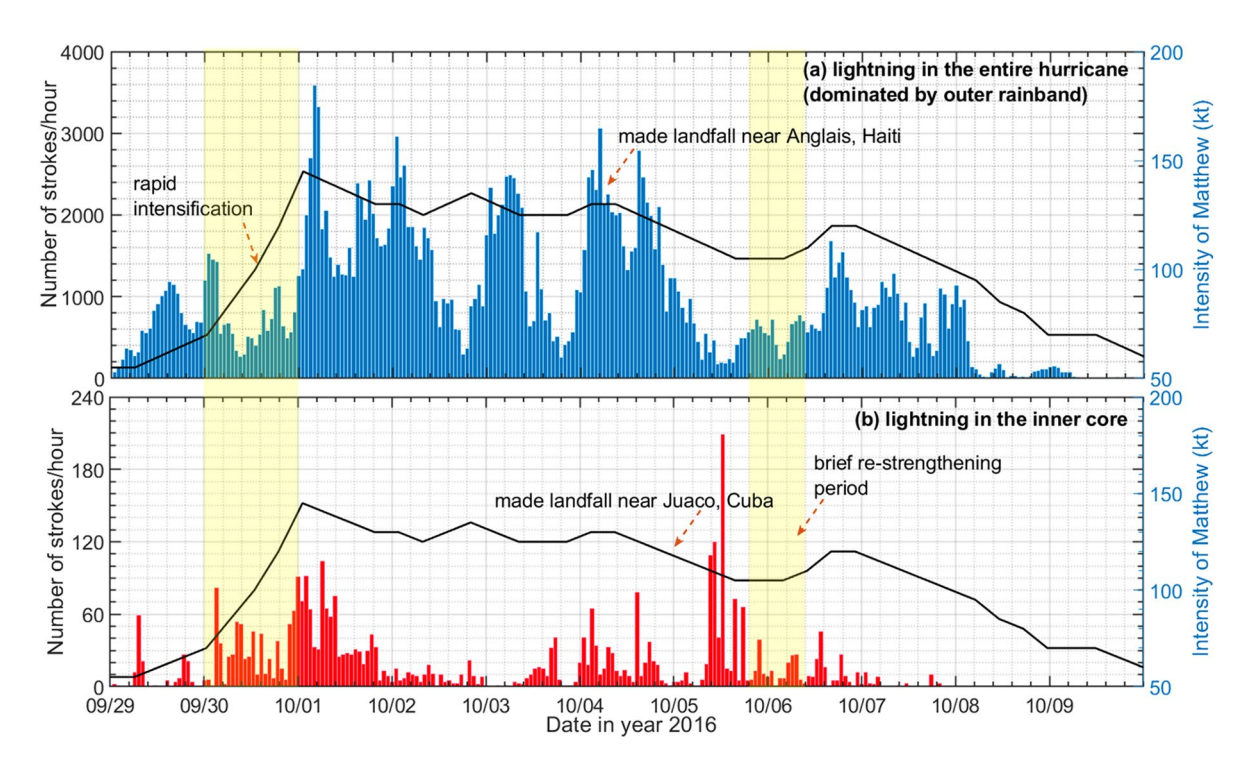


Figure 2. Comparison of the evolution of lightning activity and Matthew intensity in the entire hurricane (dominated by lightning activities in outer rainband) and the inner core region. The black curves in both panels show the variation of hurricane intensity. The histogram shows the occurrence rate of WWLLN-registered lightning discharges in the entire area (panel a) and inner core region (panel b) of Matthew hour by hour, respectively. All the time and data are UTC here. The yellow, semi-transparent rectangle highlight the period of rapid intensification from 0000 UTC September 30 to 0000 UTC October 1. Matthew made landfall near Les Anglais, Haitiat at 1100 UTC October 4 and made landfall near Juaco, Cuba at 0000 UTC October 5.

Beach. The camera had to be turned off before the thunderstorm and did not come back up until October 7. While the camera in Gainesville only showed cloudy/rainy skies, no evidence was found for sprite production above Matthew in the LMA observations. We expected to have some insights into the inner core region. However, the inner core of Matthew kept distances from the LMA network thus no related results were discussed here.

2.2. Data for Synoptic Background Analysis

In order to identify the synoptic background that can affect the temporal evolution and spatial distribution of halo/sprite-producible lightning strokes during the lifetime of Matthew, we further referred to the satellite data and the atmospheric reanalysis data.

We used the global ($60^{\circ}\text{S}-60^{\circ}\text{N}$) infrared (IR) brightness temperature data (equivalent temperature of blackbody, TBB, with a spatial resolution of 4×4 km and a temporal resolution of 30 min) merged from all available geostationary satellites (GOES-13/14/15/16 and METEOSAT-10) (Janowiak et al., 2017) over the time period of Matthew lifetime to analyze the parent thunderstorm. By overlapping the lightning data on TBB images, we could examine the hourly evolution of lightning activity during the lifetime of Matthew.

We also referred to the global atmospheric reanalysis data from Europe Center Medium-Range Weather Forecasts (ECMWF) of version Cycle 41r2, including the vertical wind velocity and cloud water data, to understand the convective structure in different regions (i.e., inner core and outer rainband) of Matthew. The reanalysis data are produced from a data assimilation system that includes a four-dimensional (4D) variational analysis with a 12 h analysis window. The horizontal spatial resolution of this dataset is about 9 km (Siemen et al., 2016) within the typical size of storm-scale structures.

HUANG ET AL. 4 of 15

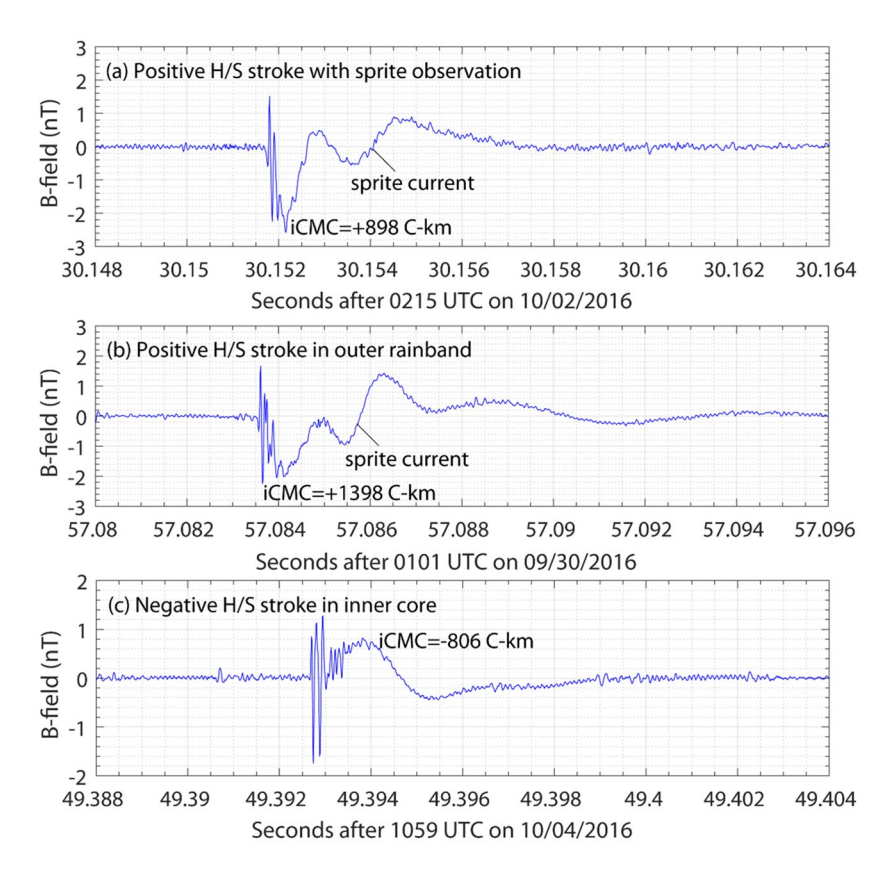


Figure 3. VLF signals recorded in Duke Forest for the lightning discharges detected by WWLLN. (a) The waveform of a positive sprite-producing stroke captured during the sprite optic observation period, which is followed by the signal from the sprite current. The iCMC value of the parent strike exceeded +800 C km; (b) Lightning waveform of a selected inner core SP + CG, which has consistent feature of (a) (i.e., distinct sprite current and iCMC >+800 C km); (c) Lightning waveform of a selected inner core SP-CG, whose duration sustained longer than 1 ms and the iCMC value exceeded -800 C km (the only H/S stroke reached the criteria (|iCMCs| > 500 C km and duration >1 ms) required for producing negative sprite).

3. Identification of Halo/Sprite-Producible Lightning Strokes

The broadband sferic signals recorded by both Duke VLF and ULF sensors can be used to evaluate the magnitude of impulse charge transfer in lightning strokes, such as impulse charge moment change (iCMC), which is defined as the product of the cloud charge removed in the first 2 ms after return stroke onset and the mean height of charge removal region. In our previous work, iCMCs have been used as a reliable metric to evaluate the capacity of sprite production by certain strokes (e.g., Cummer & Inan, 2000; Cummer & Lyons, 2005). In some cases where the luminosity of sprite is high enough with a large volume (Cummer et al., 1998; Lu et al., 2013), sprite current signal could also be considered as evidence of sprite production. For the convenience of discussion, we referred to these intense lightning strokes that could have produced halo and/or sprite as H/S strokes. Here we did not consider elves because this paper focuses on the iCMCs. Elves are always associated with large peak current strokes, which do not always have high iCMCs (Lu et al., 2013).

As Matthew mainly spent its lifetime over ocean, it is difficult to conduct a continuous observation during its life cycle. Fortunately, the existing work, both experimentally and theoretically, indicates that the typical critical charge moment changes for the production of positive and negative sprites are around +320 C km and -500 C km, respectively (e.g., Li et al., 2012; Lu et al., 2013; Qin et al., 2013); under favorable ionospheric conditions, the thresholds could drop to +200 C km and -320 C km (Qin et al., 2012). Huang, Lu, Yue et al. (2018) has examined a flash produced by Matthew. This flash has three strokes but only the first two whose iCMCs are higher than +250 C km have succeeded in producing sprites (refer to Figure 3 of Huang, Lu, Zhang et al. (2018) for more details). Therefore, the threshold for the prompt sprite production

HUANG ET AL. 5 of 15



of positive CG strokes is estimated to be between +250 and +350 C km for Matthew on October 1. Here we considered sprite and halo as the similar phenomena associated with the lightning-induced dielectric breakdown in the mesosphere. According to Lu et al. (2018), there is no considerable polarity dependence for halo production. Without losing generality, we chose |200|C km (for favorable condition) and |300| C-km (for normal condition) as the threshold to identify the lightning strokes that could produce halo and/or sprite events. These identified lightning strokes are referred to as halo/sprite-producible strokes (or H/S strokes).

We applied the iCMC criterion to the WWLLN strokes occurring in the hurricane-impacted area during the nighttime (from 0000 UTC to 1200 UTC due to the local time difference) of individual days from September 30 (only negligible strokes with estimated |iCMC| greater than 200 C km on September 28 and 29) to October 9, 2016. It should be mentioned that the aforementioned method is not guaranteed to identify all the halo/sprite events that have been produced above Matthew during its lifetime. If we consider the optical observations on October 1 and 2 (Huang, Lu, Yue et al., 2018) as truth, the false alarm rate of our method is 30.23%, suggesting that our method can capture most halo/sprite-producible strokes in Matthew.

Figure 3 shows one case of positive sprite-producible stroke captured by the camera and two cases of identified H/S strokes according to the magnetic field measurements. The first case (Figure 3a) was observed at 0215:30 UTC on October 2, and the VLF sferic waveform shows a distinct "sprite current" feature indicative of a bright sprite event (Cummer et al., 1998; Hager et al., 2012; Pasko et al., 1998). The similar feature was also observed for the inferred sprite event associated with a positive stroke (Figure 3b) detected by WWLLN in the outer rainband region at 0101:57 UTC on September 30. For the inferred negative H/S stroke shown in Figure 3c, the iCMC was calculated to be -806 C km. Note the duration of this parent lightning impulse is relatively long (approximately 2 ms), which is considered sufficiently long for the development of negative downward streamers (Li et al., 2012).

4. Evolution of H/S Strokes During the Lifetime of Matthew

By calculating the iCMCs of WWLLN strokes located in the inner core and outer rainband regions, we compared the temporal variation in the distribution of H/S strokes in various regions of Matthew during its lifetime. Special attention is paid to the behavior of negative H/S strokes because no negative sprites were captured in the optical observations (Huang, Lu, Yue et al., 2018).

4.1. Relationship Between Convection and H/S Stroke Occurrence

We compared Figures 2 and 4 to analyze the differences between lightning and H/S strokes. As shown in Figure 2, a rapid increase of the overall lightning in Matthew occurred before the RI (from 0000 UTC September 30 to 0000 UTC October 1), consistent with previous studies that the increase in lightning activity advances the maximum hurricane intensity with 1-2 days (e.g., Price et al., 2009). Both the overall and inner core lightning peaked just after the RI. In contrast, although the positive outer-rainband H/S strokes peaked at the start of RI, both positive and negative H/S strokes in the outer rainband decreased after Matthew reached the maximum intensity. Specifically, the peak of H/S strokes in the outer rainband occurred on October 2, approximately lagged one day after the maximum hurricane intensity and the maximum amount of negative inner-core H/S strokes. This time difference might imply that the formation of most negative H/S strokes in Matthew needs about 1 day after the maximum hurricane intensity for developing extensive charge distribution. Additionally, the time lag between maximum inner core and outer rainband H/S strokes could indicate that the charge transfer between these two regions causes this time difference. The intense convection activity is vortical "hot tower," which especially describes deep tropical convection in the inner core region (Riehl & Malkus, 1958). After the RI, the strong "hot power" in RI produced abundant strong lightning in the inner core (Houze, 2010), thus the amount of inner-core H/S strokes peaked after the RI. But the charges produced by this strong convection in the inner core need time to be transferred to the outer rainband. Purwado (2020) developed a method to estimate the arrival time of the latent heat energy of hurricanes and they found the energy needs 1-2 days to travel from the lightning location to the hurricane center. Therefore, the transfer of charges in the energy circulation might cause the time delay of peak H/S strokes between the inner core and outer rainband.

HUANG ET AL. 6 of 15

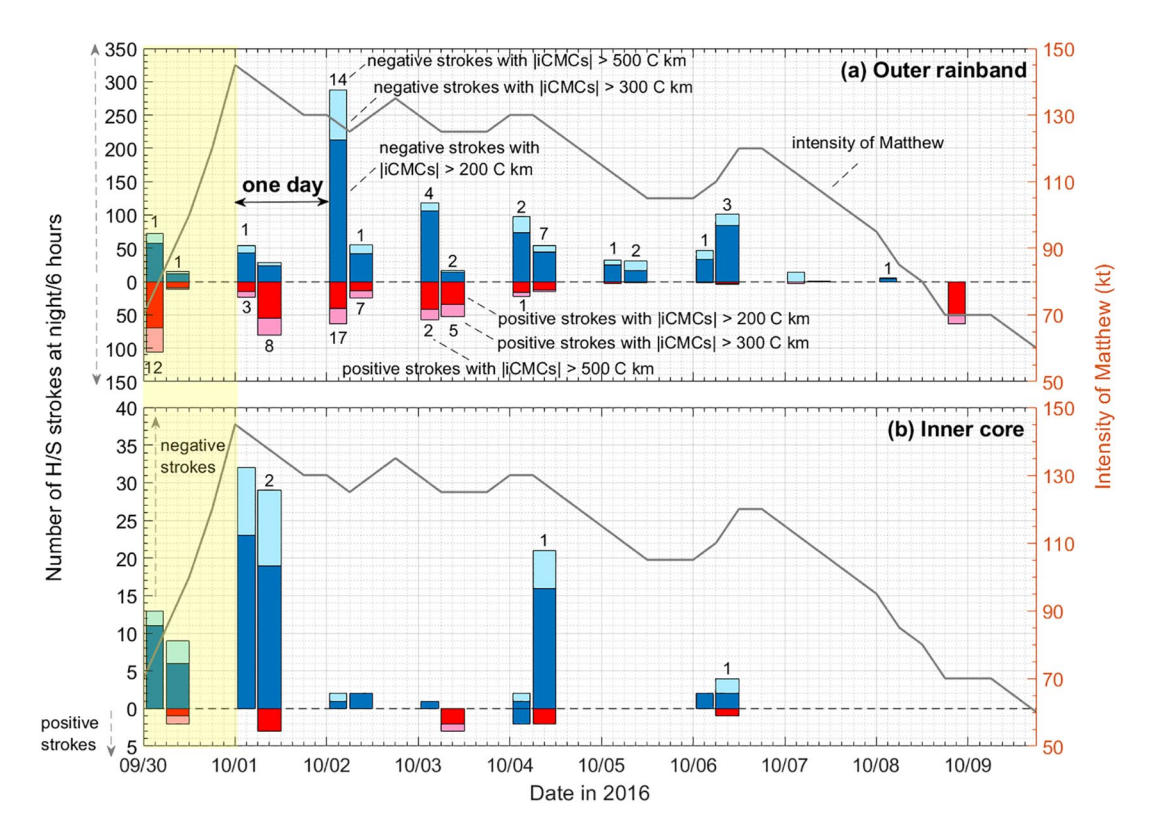


Figure 4. Numbers of H/S strokes (blue and red histograms) identified in the outer rainband (upper panel a) and inner core (lower panel b) of Hurricane Matthew (2016) in comparison with the variation of the hurricane intensity (gray curves). As indicated by the dashed arrow at the left, the up direction and down direction in *y*-axis represent the number of negative H/S strokes and positive H/S strokes, respectively. The numbers on the bars are the amounts of H/S strokes whose |iCMCs| > 500 C km at that time. All the time and data are UTC here. The number of H/S strokes is counted per 6 h and a totally of 12 h every night. The yellow, semi-transparent rectangle highlight the period of rapid intensification.

In addition, we can see the outer-rainband lightning and H/S strokes activities became relatively synchronized after October 2. The maximum difference between the outer-rainband lightning and H/S strokes occurred when Matthew reached the maximum intensity. Ringhausen and Bitzer (2021) and Bruning and MacGorman (2013) used the data from Geostationary Lightning Mapper (GLM) and LMA to suggest that when a hurricane intensifies, more turbulence will be created. The turbulence will create small pockets of charges, which support the increase in number but decrease in the size of lightning. Therefore, we could suggest the large charge reservoirs are crucial for the formation of H/S strokes. The excessively intense convective structure within Matthew may disturb the large charge reservoirs in the hurricane (Zheng et al., 2018). The restriction of the discharge area may also be responsible for the relative scarcity of H/S strokes in the outer rainband when Matthew reached the peak intensity. Although Boggs et al. (2016) suggested that one of the controlling factors of negative H/S production is intense convection, the most negative strokes with high peak current produced in the inner core probably remained impotent to produce sprites due to the relatively short charge transfer time (less than 1 ms). Therefore, despite a higher proportion of negative sprites observed over the ocean, the dynamic structure within TCs, especially in the inner core regions, may not be ideal for sprites production (Huang, Lu, Yue et al., 2018).

As shown in Figure 2, at 1100 UTC October 4 and 0000 UTC October 5, Matthew made landfall near Anglais, Haiti and near Juaco, Cuba, respectively. The land surface made lightning sharply decrease. The first landfall greatly re-boosted the amount of inner-core H/S strokes. Nonetheless, this landfall did not produce a considerable impact on the H/S strokes spawned in the outer rainband. It's obvious the landfalls will largely influence both the lightning and H/S strokes. But the detailed effects from landfalls are very complicated and we will not discuss them in the paper without supports from observations.

Shortly after the second landfall, the eye region of Matthew expanded and split into double eyewalls (Miller et al., 2018) and Matthew experienced a brief re-strengthening period from 1800 UTC October 5

HUANG ET AL. 7 of 15

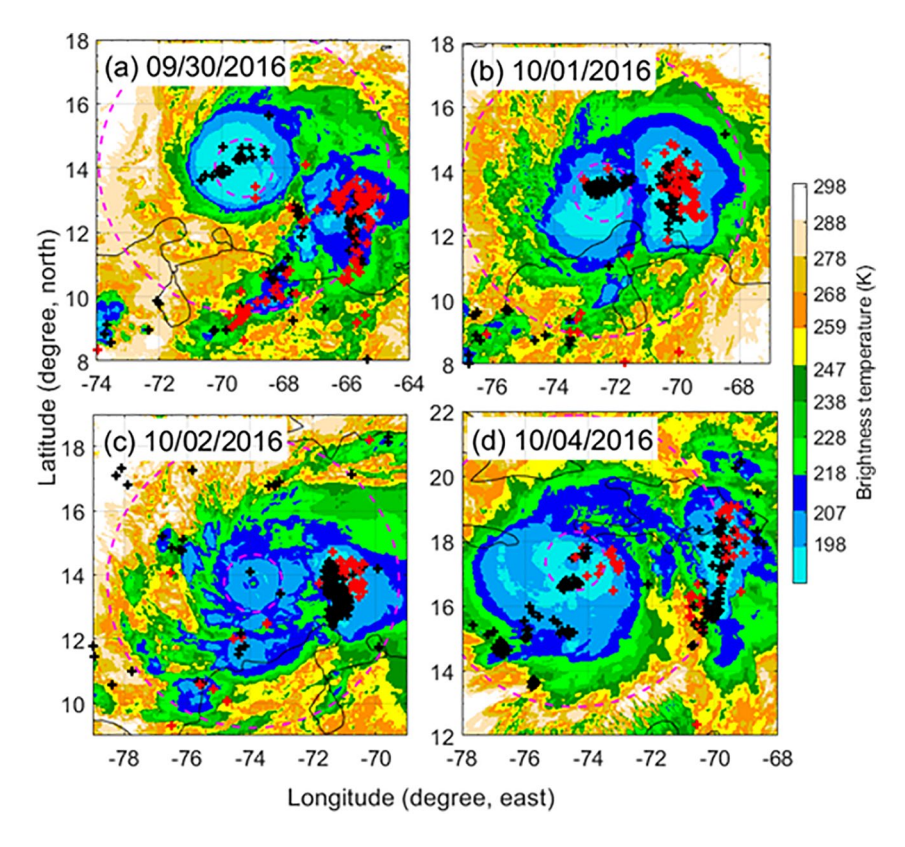


Figure 5. Distribution of H/S strokes in comparison with the satellite data at four selected dates. We selected the middle time as 0300 UTC of each night. The red pulses represent the positive H/S strokes and the black pluses represent the negative H/S strokes. The two pink dashed circles define the peripheries of the inner core (0–100 km) and out rainband (>100 km) regions with Matthew. The inner core of Matthew was dominated by negative H/S strokes. Both positive and negative H/S strokes are found in the outer rainband region.

to 0600 UTC October 6. Although the inner-core lightning increased sharply to the maximum before the re-strengthening period, no inner-core H/S strokes occurred in the meantime. The lack of H/S strokes even when the lightning activities were still vigorous at the later stage of Matthew may suggest the sufficient strong intensity of the hurricane is essential for the formation of H/S strokes.

In summary, for the entire hurricane, the intense convection during the RI indeed contributes greatly to enhance the lightning density but the phase about 1 day after the RI is more favorable to negative produce H/S strokes.

4.2. Spatial Distribution of H/S Strokes

In Figure 5, the TBB images were selected at 0600 UTC on each day, and the H/S strokes were identified from 0000 UTC to 1200 UTC on the same day. Positive and negative H/S strokes were indicated by red pluses and black pluses, respectively. The inner core was usually dominated by negative H/S strokes, and the positive counterparts were very rare. In the outer rainband, both positive and negative H/S strokes could be found. Moreover, the positive H/S strokes tended to be located toward the peripheral region of outer rainband.

In addition, the distribution of H/S strokes in the outer rainband was relatively expansive, which may imply an extensive distribution of positive and negative charges over a lateral scale of 200 km in this region. In fact, the morphology (including spatial scale and shape factor) of sprites to some extent also reflects the lightning progression inside parent thunderstorms (e.g., Lu et al., 2013). Figure 6 shows the composite image for a sprite observed at 0529:11 UTC on October 1st. By placing the center of these sprite elements right above the parent stroke located by WWLLN (at 14.3161°N, 70.0415°W), the transversal scale of this

HUANG ET AL. 8 of 15

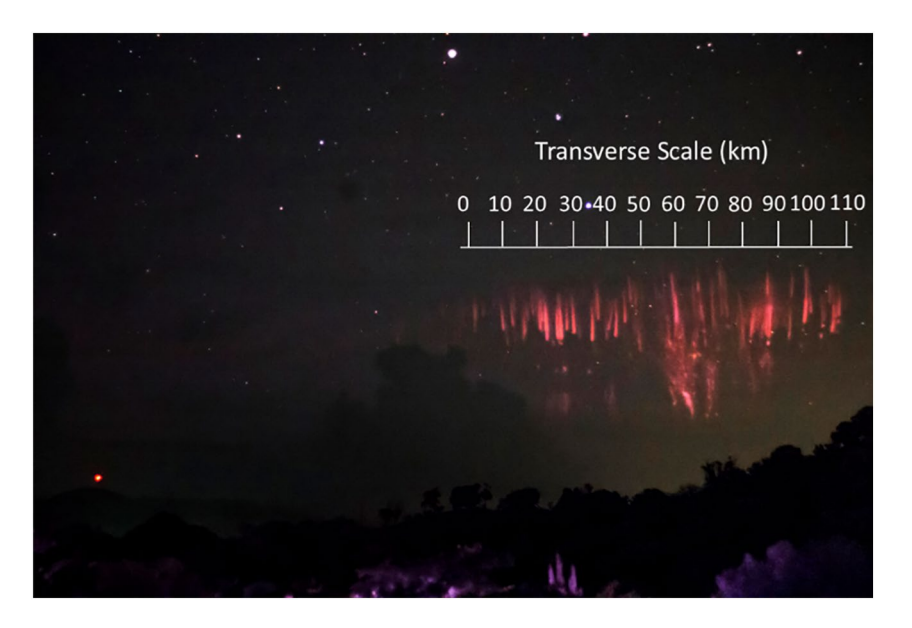


Figure 6. Composite image of an extensive sprite cluster captured from Puerto Rico on October 1, 2016. The sprite event consists of nearly 30 sprite elements produced by three lightning strokes that each produces an iCMC greater than +300 C km, and the second stroke was detected by WWLLN at 0529:11.140 UTC.

sprite was estimated to be more than 100 km (by comparing with the starfield) which is greater than the maximum size of all the sprites observed over an MCS observed by Lu et al. (2013) in the central plain of United States. For the observations over continental MCSs, the transverse scale of sprites produced by individual flashes usually ranges from 10 to 50 km, although occasionally the cluster of sprite elements (in the so-called dancing sprites) can span up to 200 km (Lyons & Keen, 1994).

5. Characteristics of H/S Strokes in the Inner Core

The inner core of hurricanes is a characteristic region with deep, episodic and weakly electrified oceanic convection. Most previous studies focus on the relationship between inner-core lightning and TC intensity (e.g., Fierro & Mansell, 2017; Price et al., 2009). As an independent warm thundercloud system that is mainly controlled by the central rotational angular power (Houze, 2010), the lightning burst in the inner core has been associated with intensity changes of TCs. The changes most tend to occur before or during the RI period of TCs in the Atlantic Ocean.

Thomas et al. (2010) examined three cases of Atlantic hurricanes in 2005, without finding evidence for the considerable sprite production over the inner core of these cases. This is confirmed by the case study of Matthew by Huang, Lu, Yue et al. (2018). Only one sufficient long, negative H/S stroke reached the criteria (|iCMCs| > 500 C| km and duration > 1 ms) required for producing a negative sprite as introduced in Figure 3c of Section 3; this event was found on October 4 after the first landfall. However, as the halo production only requires a sufficiently large impulsive charge transfer (e.g., |iCMC| > 300 C| km) other than a supportive long period (Lu et al., 2018), it remains possible for the active halo production over the inner core of Matthew. During the major life cycle of Matthew, there were a totally of 112 H/S strokes (|iCMC| > 200 C| km) identified in the inner core region, with about 89% being negative.

To get more insights into the temporal variation of the population of negative H/S strokes in the inner core of Matthew, we referred to the reanalysis results of ECMWF modeling to discuss its vertical wind configuration. The melting isotherm (0°C) was located at around 550 hPa, roughly 5 km according to the nearby sounding results. Figure 7 shows the profile of vertical wind velocity on three representative times: October 1, 3, and 4, respectively. The vertical wind velocity was retrieved from the ECMWF reanalysis data. On October 1, Matthew just ended the RI and its intensity reached the maximum. A large quantity of H/S strokes was found in the inner core. We selected two representative locations whose longitudes are at the center and the

HUANG ET AL. 9 of 15

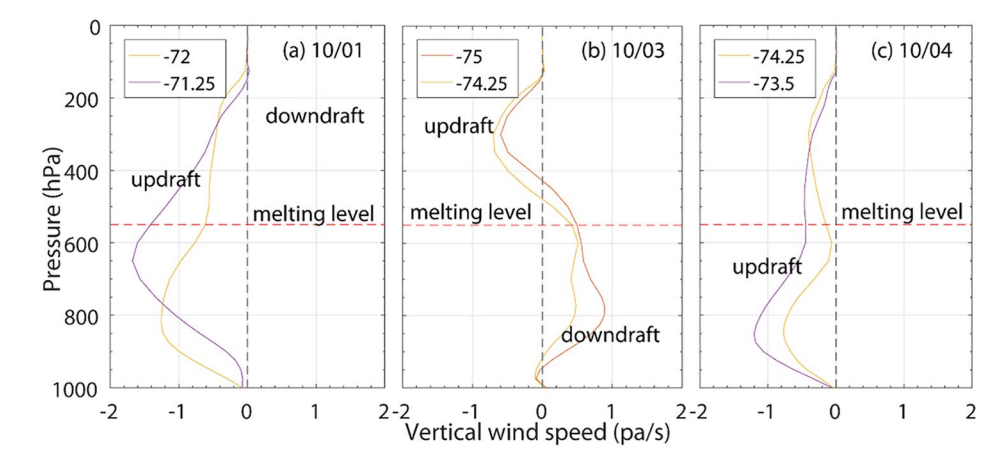


Figure 7. Vertical wind profiles from two representative locations (the legend of each panel shows the longitude; the latitude is consistent with the center of Matthew) in the inner core of Matthew on October 1, 3, and 4, respectively. In the pressure coordinate system, the updraft corresponds to the negative vertical wind speed and the downdraft corresponds to positive vertical wind speed. Bursts of H/S strokes were found in the inner core on October 1 and October 4. Not many H/S strokes were found in the inner core on October 3 when Matthew still kept strong intensity.

edge of the inner core and latitudes are at the center of the inner core to examine the vertical wind profile. On October 1, the inner core was dominated by updraft from the ground to the upper level, and the strongest updraft was located below the melting level, matching the maximum center of liquid water content (also retrieved from the ECMWF data but is not shown here). Under this configuration, the strong updrafts will easily bring liquid water to the upper level for the super-cooled water production (Carey et al., 2005). This configuration can be supported by the "cloud invigoration" theory, which suggested that when the warm rain process was suppressed, more liquid water would be permitted to reach the freezing level and thereby enhance the latent heat release in the upper portion of clouds (Khain et al., 2005; Rosenfeld et al., 2008). Above the melting level, the updraft speed decreases with height. Therefore, the ice splinters could grow by collection and began to spread out with the tangential velocities due to the weakening vertical wind at high levels (Takahashi, 1982). We can safely speculate that these ice particles will keep falling until they encounter strong updrafts with super-cooled water content at the lower level. Boggs et al. (2016) also examined two negative sprite-producing thunderstorms associated with a tropical disturbance but not TCs. They suggested that the strong wind shear at middle to upper levels of tropical thunderstorms would enhance the downward transfer of negative charges because the tiled and rearranged turbulent mixing will reduce the upper positive charge. Therefore, the special warm cloud traits of the inner core result in a unique favorable convective structure for the formation of H/S strokes. However, this favorable structure is usually not satisfied of inner core due to its relatively weak convection during most time compared to the outer rainband (Fierro & Mansell, 2017).

For comparison, we also examined the wind profile on October 3 when the hurricane remained strong but no positive H/S strokes were found in the inner core. Compared to October 1, the vertical wind speed decreased on October 3, and the downdrafts dominated from the ground to 400 hPa, sharply suppressed the growth of hydrometeors. The weak updraft existed at a high level matching the ice water content (retrieved from the ECMWF data but is not shown here), which could favor the growth of ice particles. However, this vertical wind distribution may not provide enough mixed-phase particles for discharges due to insufficient super-cooled water supplied from low levels (Baker et al., 1999).

On October 4, the inner core H/S strokes were substantially produced when the updrafts dominated the vertical wind field at low levels of the inner core again. In addition, the maximum wind speed was located even lower compared to October 1.

From the similar vertical wind distribution on October 1 and 4, we suggest that the dominance of updrafts at low levels is critical for H/S strokes production. The charge separation per collision highly depends on the super-cooled water content (Saunders et al., 1991). In the inner core area, the super-cooled liquid water was confined to a narrow region on the inward edge of the eyewall (Black & Hallett, 1999). The graupel particles,

HUANG ET AL. 10 of 15



which are heavier than cloud ice, are often found at low altitudes (Barthe et al., 2016; Houze, 2010). Thus the inner core could be most electrically active due to abundant falling ice particles encountering the strong updraft at low levels (Warner, 1970), which lifted the grapple and super-cooled water (Cecil & Zipser, 2002; Reinhart et al., 2014). Fierro and Mansell (2017) also reported that the moderate updraft speeds (about 5 m/s) in the inner-core convection is located at relatively lower levels compared to the outer rainband.

In summary, the H/S strokes in the inner core of Matthew appeared to form in the strong updrafts-dominated environment while the updraft speeds peaked at low levels (at about 3.5 km) corresponding to the maximum liquid water content. Lightning is produced above the altitude of zero isotherms with critical electric fields related to cloud size and convection. Compared to the continental MCS, the hurricane has relatively lower cloud base and higher ice-forming level. There is a broader space for the development of the inner core clouds. The convective inner core clouds might grow vigorously and reach the critical size for lightning producing below the altitude of zero isotherms. Therefore, the critical condition for electrification in the warm cloud is that the super-cooled water could be rapidly lifted by profound updrafts at low levels and could escape from being depleted by active conversion and accretion (e.g., warm rain) processes (Barthe et al., 2016).

6. Comparison of Outer Rainband With Continental Sprite-Producing MCSs

In this section, we compared the outer rainband with the continental MCSs. MCSs are the typical sprite-producing thunderstorms with parent lightning strokes (SP + CGs) located in the trailing stratiform region (e.g., Boccippio et al., 1995; Huang, Lu, Zhang et al., 2018; Lu et al., 2013; Soula et al., 2009; Yang et al., 2013). The outer rainband region easily deviates from the control of the hurricane eye and exchanges momentum with the environmental air. Thus, the outer rainband can be strongly influenced by the ambient unstable environment, which can provide sufficient updrafts for the charge separation. Eventually, the outer rainband may gradually separate from the principal part of the hurricane and could resemble the trailing stratiform region of MCS.

6.1. Amounts of H/S Strokes During the Dissipation Stage of Matthew

During the dissipation stage of Matthew (since the morning of October 7), as shown in Figure 4, there were no observations of H/S strokes in the inner core. The H/S strokes in the outer rainband were first dominated by negative strokes and then decreased sharply. Note that at the end of Matthew, there was a sudden increase of the positive H/S strokes in the outer rainband while the outer-rainband lightning is sparse in Figure 2a. Boggs et al. (2018) also observed the overall decreasing lightning activities are often accompanied by the enhanced proportion of positive strokes. In the dissipation stage, the outer rainband can obtain exuberant momentum under the influence of the environmental air when the dynamic center of Matthew gradually loses control. Thus, the outer rainband becomes more similar to the continental MCS. The previous studies of continental MCSs have suggested that most sprites are associated with positive SP + CGs occurring during the MCS's mature-to-late stages (Lu et al., 2013; Savtchenko et al., 2009), especially by the long-duration flashes that tend to occur in the dissipation stage of MCSs (Albrecht et al., 2011; Peterson & Liu, 2011). Therefore, at the dissipation stage of the outer rainband, although the overall activities of lightning weakened, the proportion of positive CGs and precipitation clouds was enhanced, maintaining the high productivity of H/S strokes (Lu et al., 2009).

In contrast, the development of outer rainband will constrict the intensity of the static wind center (eye region) and thus there is no more evident ability of the inner core to produce transient luminous events above the thunderstorm in the dissipation stage.

6.2. Segregation of Positive and Negative H/S Strokes in the Outer Rainband

As discussed in Section 6.1, when the hurricane intensity decreases, the H/S strokes in the outer rainband have a higher proportion of positive CG strokes. Moreover, compared to the discussion of the entire hurricane in Section 4.2, the positive strokes were mostly located radially outward from the cluster of neg-

HUANG ET AL. 11 of 15



ative strokes (Molinari et al., 1994, 1999; Zhang et al., 2012), and formed an overall bi-pole structure in the outer rainband.

Orville et al. (1988) reported the bi-pole pattern of lightning strokes spawned by MCSs, namely the positive and negative strokes appear to dominate in two different regions of MCSs with a characteristic separation of about 100 km. Orville et al. (1988) indicated that this pattern aligned with the directional shear at the upper level. Corbosiero and Molinari (2002) also suggested that the vertical wind shear will influence the convective asymmetries, which will further lead to the asymmetries of electrification. The low-pressure center of Matthew was probably tilted southeast at the higher levels (especially above 650 hPa) with directional wind shear. The tilted eyewall, which contains fruitful updrafts, can contribute to the charge separation process. The large-scale charge separation will place the region of positive flash outward of negative flash (Zhang et al., 2012).

The outer rainband has some characteristics of the trailing stratiform region of MCSs which include most SP strokes of the storms and a high proportion of positive strokes (Molinari et al., 1999). Once the hydrometeors rapidly electrified in the eyewall fall out, they melt into the stratiform precipitation far away. Therefore, the outer rainband is dominated by stratiform with several convection cells (Cecil & Zipser, 2002). Furthermore, after Matthew made landfall on October 4, the outer rainband gradually separated from the inner core due to the significant friction with the surrounding environment. Consequently, the outer rainband largely resembled the trailing stratiform region of continental MCS reported in Huang, Lu, Zhang et al. (2018) with abundant SP strokes, especially SP + CGs, crowded in the vast precipitation cloud (Lyons & Keen, 1994; Molinari et al., 1999).

However, the SP + CGs were produced in the outer rainband region of Matthew where cloud top temperature ranges from 183 to 194 K (Huang, Lu, Yue et al., 2018). While the typical coldest cloud top temperature of sprite-producing MCS is 205 K (Huang, Lu, Zhang et al., 2018; Soula et al., 2009). Braga and Vila (2014) suggested that the threshold for ice production near the cloud top is 233 K. Therefore, the thunderstorm region hosting sprite-producing strokes in Matthew developed higher with colder cloud top temperatures compared to the continental MCS. Strong convective cells of Matthew highly probable contain accumulated ice near the cloud top.

Additionally, the similarity between outer rainband and trailing stratiform regions of MCSs may be caused by the tilt of the eyewall (Marks & Houze, 1987), which produced the lateral displacement of the upper positive charge layer and the middle negative layer. This tilted dipole cloud configuration will benefit the production of positive lightning (Nag & Rakov, 2012) and most positive lightning occurred in the stratiform regions (Molinari et al., 1999; Lyons & Keen, 1994).

7. Conclusions

In this paper, we examined the evolution of intense CG strokes (iCMCs > |200|C km) that are inferred to be capable of producing halos and/or sprites during the lifetime of hurricane Matthew (2016). In this way, we could obtain a general idea about the halo/sprite production of tropical cyclones as the characteristic large-scale thunderstorm in the ocean. In comparison with the analysis of Thomas et al. (2010), we extended the investigation from the inner core to the outer rainband region, confirming that the outer rainband is a productive area of positive halo/sprite and is similar to the trailing stratiform region of continental MCSs.

The inner core area also has a significant impact on the lower ionosphere through spawning a large amount of negative halo-producing strokes. In general, the inner core bears more features that merit further investigations into the relatively high population of negative halos or sprites in the ocean as indicated by the space-born observations (Lu et al., 2017). For example, the presence of updraft below the melting level in the inner core could be essential for the formation of halo/sprite producible strokes, different from the normal oceanic storms which need intense convection above the melting level to produce halo/sprite producible strokes (Boggs et al., 2016). In addition, the postponement of the peak time of H/S strokes in the outer rainband compared to the inner core might support the conjecture that the electric charge in the outer rainband resulted from the advection of convection in the inner core, which is the dominant thermo-dynamical structure in the formation of tropical cyclone (Houze, 2010).

HUANG ET AL. 12 of 15



In contrast, the outer rainband of Matthew is similar to trailing stratiform regions of continental MCSs. The outer rainband could also produce a large number of sprites as continental MCSs, which was confirmed by existing observations. In addition, H/S strokes in the outer rainband also exhibit a bi-pole structure that implies a separation of extensively distributed negative and positive charges in the outer rainband. This feature is also similar to the continental MCSs.

Different from continental MCSs over which the sprite production usually persists until the dissipation stage when the positive CG flashes are particularly intense even with significantly reduced lightning activity (e.g., Lu et al., 2009), there is no considerable sprite (or halo) production in the inner core of Matthew during the dissipation stage.

Our analyses presented in this paper are mainly based on the remote sensing of broadband lightning sferics. It is certainly desired to conduct more observations over oceanic thunderstorms (including multi-cell thunderstorms and tropical cyclones), especially low-light-level optical observations with high sensitivity, to understand the relatively high population of negative sprite-producing strokes in the ocean and the properties that make the oceanic thunderstorms conducive to negative CG strokes with high peak current.

Data Availability Statement

The data examined in this paper are available at https://zenodo.org/deposit/3724824.

Acknowledgments

This work was supported by National Natural Science Foundation of China (Grant No. 41574141 and 41374153), Key Program for International Science and Technology Innovation Cooperation Projects of China (2018YFE0101200) and the International Partnership Program of Chinese Academy of Sciences (Grant No. 183311KYSB20200003). We would like to thank the World-Wide Lightning Location Network (http://wwlln.net), a collaboration among over 40 universities and institutions, for providing the lightning location data used in this paper. We also appreciate three reviewers' very helpful suggestions, which improve the paper to a better version.

References

- Abarca, S. F., Corbosiero, K. L., & Galarneau, T. J. (2010). An evaluation of the Worldwide Lightning Location Network (WWLLN) using the National Lightning Detection Network (NLDN) as ground truth. *Journal of Geophysical Research*, 115, D18206. https://doi.org/10.1029/2009JD013411
- Albrecht, R. I., Morales, C. A., & Silva Dias, M. A. F. (2011). Electrification of precipitating systems over the Amazon: Physical processes of thunderstorm development. *Journal of Geophysical Research: Atmosphere*, 116, D08209. https://doi.org/10.1029/2010jd014756
- Baker, M. B., Blyth, A. M., Christian, H. J., Lathamd, J., Miller, K. L., & Gadian, A. M. (1999). Relationships between lightning activity and various thundercloud parameters: Satellite and modelling studies. *Atmospheric Research*, 51(3), 221–236. https://doi.org/10.1016/s0169-8095(99)00009-5
- Barthe, C., Hoarau, T., & Bovalo, C. (2016). Cloud electrification and lightning activity in a tropical cyclone-like vortex. *Atmospheric Research*, 180, 297–309. https://doi.org/10.1016/j.atmosres.2016.05.023
- Black, R. A., & Hallett, J. (1999). Electrification of the hurricane. *Journal of the Atmospheric Sciences*, 56, 2004–2028. https://doi.org/10.1175/1520-0469(1999)056<2004:eoth>2.0.co;2
- Boccippio, D. J., Williams, E. R., Heckman, S. J., Lyons, W. A., Baker, I. T., & Boldi, R. (1995). Sprites, ELF transients and positive ground strokes. *Science*, 269, 1088–1091. https://doi.org/10.1126/science.269.5227.1088
- Boggs, L. D., Liu, N., Riousset, J., Shi, F., Rassoul, H. (2018). Thunderstorm charge structures producing gigantic jets. *Scientific Reports*, 8(1). https://doi.org/10.1038/s41598-018-36309-z
- Boggs, L. D., Liu, N., Splitt, M., Lazarus, S., Glenn, C., Rassoul, H., et al. (2016). An analysis of five negative sprite-parent discharges and their associated thunderstorm charge structures. *Journal of Geophysical Research: Atmospheres*, 121, 759–784. https://doi.org/10.1002/2015jd024188
- Braga, R. C., & Vila, D. A. (2014). Investigating the ice water path in convective cloud life cycles to improve passive microwave rainfall retrievals. *Journal of Hydrometeorology*, 15, 1486–1497. https://doi.org/10.1175/jhm-d-13-0206.1
- Bruning, E. C., & MacGorman, D. R. (2013). Theory and observations of controls on lightning flash size spectra. *Journal of the Atmospheric Sciences*, 70(12), 4012–4029. https://doi.org/10.1175/JAS-D-12-0289.1
- Carey, L. D., Murphy, M. J., McCormick, T. L., & Demetriades, N. W. S. (2005). Lightning location relative to storm structure in a leading-line, trailing-stratiform mesoscale convective system. *Journal of Geophysical Research: Atmosphere*, 110, D03105. https://doi.org/10.1029/2003jd004371
- Cecil, D. J., & Zipser, E. J. (2002). Reflectivity, ice scattering, and lightning characteristics of hurricane eyewalls and rainbands. Part II: Inter-comparison of observations. *Monthly Weather Review*, 130, 785–801. https://doi.org/10.1175/1520-0493(2002)130<0785: risalc>2.0.co;2
- Chen, A. B., Kuo, C. L., Lee, Y. J., Su, H. T., Hsu, R. R., Chern, J. L., et al. (2008). Global distributions and occurrence rates of transient luminous events. *Journal of Geophysical Research: Atmospheres*, 113, A08306. https://doi.org/10.1029/2008JA013101
- Chen, A. B.-C., Chen, H., Chuang, C.-W., Cummer, S. A., Lu, G., Fang, H.-K., et al. (2019). On negative sprites and the polarity paradox. Geophysical Research Letters, 46. https://doi.org/10.1029/2019GL083804
- Christian, H., Blakeslee, R. J., Boccippio, D. J., Boeck, W. L., Buechler, D. E., Driscoll, K. T., et al. (2003). Global frequency and distribution of lightning as observed from space by the Optical Transient Detector. *Journal of Geophysical Research: Atmospheres*, 108(D1), 4005. https://doi.org/10.1029/2002JD002347
- Corbosiero, K. L., & Molinari, J. (2002). The effects of vertical wind shear on the distribution of convection in tropical cyclones. *Monthly Weather Review*, 130, 2110–2123. https://doi.org/10.1175/1520-0493(2002)130<2110:TEOVWS>2.0.CO;2
- Cummer, S. A., & Inan, U. S. (2000). Modeling ELF radio atmospheric propagation and extracting lightning currents from ELF observations. *Radio Science*, 35, 385–394. https://doi.org/10.1029/1999rs002184
- Cummer, S. A., Inan, U. S., Bell, T. F., & Barrington-Leigh, C. P. (1998). ELF radiation produced by electrical currents in sprites. *Geophysical Research Letters*, 25(8), 1281–1284. https://doi.org/10.1029/98gl50937

HUANG ET AL. 13 of 15



- Cummer, S. A., & Lyons, W. A. (2005). Implications of lightning charge moment changes for sprite initiation. *Journal of Geophysical Research: Atmosphere*, 110, A04304. https://doi.org/10.1029/2004ja010812
- Fierro, A. O., & Mansell, E. R. (2017). Electrification and lightning in idealized simulations of a hurricane-like vortex subject to wind shear and sea surface temperature cooling. *Journal of the Atmospheric Sciences*, 74, 2023–2041. https://doi.org/10.1175/jas-d-16-0270.1
- Frey, H. U., Mende, S. B., Cummer, S. A., Li, J., Adachi, T., Fukunishi, H. et al. (2007). Halos generated by negative cloud-to-ground lightning. *Geophysical Research Letters*, 34, L18801. https://doi.org/10.1029/2007GL030908
- Hager, W. W., Sonnenfeld, R. G., Feng, W., Kanmae, T., Stenbaek-Nielsen, H. C., McHarg, M. G., et al. (2012). Charge rearrangement by sprites over a north Texas mesoscale convective system. *Journal of Geophysical Research: Atmosphere*, 117, D22101. https://doi. org/10.1029/2012jd018309
- Houze, R. A. (2010). Clouds in tropical cyclones. Monthly Weather Review, 138(2), 293-344. https://doi.org/10.1175/2009mwr2989.1
- Huang, A., Lu, G., Yue, J., Lyons, W., Lucena, F., Lyu, F., et al. (2018). Observations of red sprites above Hurricane Matthew. *Geophysical Research Letters*, 45(13), 165. https://doi.org/10.1029/2018GL079576
- Huang, A., Lu, G., Zhang, H., Liu, F., Fan, Y., Zhu, B., et al. (2018). Locating parent lightning strokes of sprites observed over a mesoscale convective system in Shandong Province, China. Advances in Atmospheric Sciences, 35(11), 1396–1414. https://doi.org/10.1007/s00376-018-7306-4
- Janowiak, J., Joyce, B., & Xie, P. (2017). NCEP/CPC L3 half hourly 4km global (60S 60N) merged IR V1. In A. Savtchenko, & M. D. Greenbelt (Eds.), Goddard earth sciences data and information services center (GES DISC). Accessed: (Data Access Date) https://doi.org/10.5067/P4HZB9N27EKU
- Khain, A., Rosenfeld, D., & Pokrovsky, A. (2005). Aerosol impact on the dynamics and microphysics of deep convective clouds. *Quarterly Journal of the Royal Meteorological Society*, 131, 2639–2663. https://doi.org/10.1256/qj.04.62
- Lay, E. H., Holzworth, R. H., Rodger, C. J., Thomas, J. N., Pinto, O., & Dowden, R. L. (2004). WWLL global lightning detection system: Regional validation study in Brazil. *Geophysical Research Letters*, 31, L03102. https://doi.org/10.1029/2003GL018882
- Li, J. B., Cummer, S., Lu, G. P., & Zigoneanu, L. (2012). Charge moment change and lightning-driven electric fields associated with negative sprites and halos. *Journal of Geophysical Research: Atmosphere*, 117, A09310. https://doi.org/10.1029/2012ja017731
- Lu, G., Cummer, S. A., Chen, A. B., Lyu, F., Li, D., Liu, F. et al. (2017). Analysis of lightning strokes associated with sprites observed from space in North America. *Terrestrial, Atmospheric and Oceanic Sciences*, 28(4), 583–595. https://doi.org/10.3319/tao.2017.03.31.01
- Lu, G., Cummer, S. A., Li, J., Han, F., Blakeslee, R. J., & Christian, H. J. (2009). Charge transfer and in-cloud structure of large-charge-moment positive lightning strokes in a mesoscale convective system. *Geophysical Research Letters*, 36, L15805. https://doi.org/10.1029/2009GL038880
- Lu, G., Cummer, S. A., Li, J., Zigoneanu, L., Lyons, W. A., Stanley, M. A. et al. (2013). Coordinated observations of sprites and in-cloud lightning flash structure. *Journal of Geophysical Research: Atmosphere*, 118, 6607–6632. https://doi.org/10.1002/jgrd.50459
- Lu, G., Yu, B., Cummer, S. A., Peng, K.-M., Chen, A. B., Lyu, F., et al. (2018). On the causative strokes of halos observed by ISUAL in the vicinity of North America. *Geophysical Research Letters*, 45(10), 789. https://doi.org/10.1029/2018GL079594
- Lyons, W. A., & Keen, C. (1994). Observations of lightning in convective supercells within tropical storms and hurricanes. *Monthly Weather Review*, 122, 1897–1916. https://doi.org/10.1175/1520-0493(1994)122<1897:oolics>2.0.co;2
- Marks, F. D., & Houze, R. A. (1987). Inner core structure of Hurricane Alicia from airborne doppler radar observations. *Journal of the Atmospheric Sciences*. (Vol. 44, pp. 1296–1317). https://doi.org/10.1175/1520-0469(1987)044<1296:ICSOHA>2.0.CO
- Miller, S., Straka, W., Yue, J., Seaman, C. J., Xu, S., Elvidge, C. D. et al. (2018). The dark side of Hurricane Matthew: Unique perspectives from the VIIRS day/night band. *Bulletin of the American Meteorological Society*, 99, 2561–2574. https://doi.org/10.1175/bams-d-17-0097.1
- Miyasato, R., Taylor, M. J., Fukunishi, H., & Stenbaek-Nielsen, H. C. (2002). Statistical characteristics of sprite halo events using coincident photometric and imaging data. *Geophysical Research Letters*, 29(21), 2033. https://doi.org/10.1029/2001GL014480
- Molinari, J., Moore, P., Idone, V., Nag, A., & Rakov, V. A. (1999). Convective structure of hurricanes as revealed by lightning locations. *Monthly Weather Review. Journal of Geophysical Research*, 127, 520–534. https://doi.org/10.1029/2012JD01754510.1175/1520-0493(1999)127<0520:csohar>2.0.co;2
- Molinari, J., Moore, P. K., Idone, V. P., Henderson, R. W., & Saljoughy, A. B. (1994). Cloud-to-ground lightning in Hurricane Andrew. *Journal of Geophysical Research*, 99, 676. https://doi.org/10.1029/94jd00722
- Nag, A., & Rakov, V. A. (2012), Positive lightning: An overview, new observations, and inferences, *Journal of Geophysical Research*, 117, D08109. https://doi.org/10.1029/2012JD017545
- Orville, R. E., Henderson, R. W., & Bosart, L. F. (1988). Bipole patterns revealed by lightning locations in mesoscale storm systems. *Geophysical Research Letters*, 15, 129–132. https://doi.org/10.1029/gl015i002p00129
- Pasko, V. P., Inan, U. S., Bell, T. F., & Reising, S. C. (1998). Mechanism of ELF radiation from sprites. *Geophysical Research Letters*, 25(18), 3493–3496. https://doi.org/10.1029/98gl02631
- Peterson, M., & Liu, C. (2011). Global statistics of lightning in anvil and stratiform regions over the tropics and subtropics observed by the Tropical Rainfall Measuring Mission. *Journal of Geophysical Research*, 116, D23201. https://doi.org/10.1029/2011jd015908
- Price, C., Asfur, M., & Yair, Y. (2009). Maximum hurricane intensity preceded by increase in lightning frequency. *Nature Geoscience*, 2, 329–332. https://doi.org/10.1038/ngeo477
- Purwado, P. (2020). AE011-08 Correlation between typhoon-related lightning activity and the maximum wind speed near the center examined by back-tracing technique [Oral presentation] AGU fall meetingThunderstorm Electrification and Lightning Meteorology section. online.
- Qin, J., Celestin, S., & Pasko, V. P. (2012). Minimum charge moment change in positive and negative cloud to ground lightning discharges producing sprites. *Geophysical Research Letters*, 39, L22801. https://doi.org/10.1029/2012gl053951
- Qin, J., Celestin, S., & Pasko, V. P. (2013). Dependence of positive and negative sprite morphology on lightning characteristics and upper atmospheric ambient conditions. *Journal of Geophysical Research: Space Physics*, 118, 2623–2638. https://doi.org/10.1029/2012ja017908
- Qin, J. Q., Pasko, V. P., McHarg, M. G., & Stenback-Nielsen, H. C. (2014). Plasma irregularities in the D-region ionosphere in association with sprite streamer initiation. *Nature Communications*, 5, 3740. https://doi.org/10.1038/ncomms4740
- Reinhart, B., Fuelberg, H., Blakeslee, R., Mach, D., Heymsfield, A., Bansemer, A. et al. (2014). Understanding the relationships between lightning, cloud microphysics, and airborne radar-derived storm structure during Hurricane Karl (2010). *Monthly Weather Review*, 142, 590–605. https://doi.org/10.1175/mwr-d-13-00008.1
- Riehl, H., & Malkus, J. S. (1958). On the heat balance in the equatorial trough zone. Geophysica, 6, 503-538.
- Ringhausen, J. S., & Bitzer, P. M. (2021). An in-depth analysis of lightning trends in hurricane harvey using satellite and ground-based measurements. *Journal of Geophysical Research: Atmospheres*, 126(7), 1–26. https://doi.org/10.1029/2020JD032859

HUANG ET AL. 14 of 15



- Rosenfeld, D., Lohmann, U., Raga, G. B., O'Dowd, C. D., Kulmala, M., Fuzzi, S., et al. (2008). Flood or drought: How do aerosols affect precipitation? *Science*, 321(5894), 1309–1313. https://doi.org/10.1126/science.1160606
- Said, R. K., Cohen, M. B., & Inan, U. S. (2013). Highly intense lightning over the oceans: Estimated peak currents from global GLD360 observations. *Journal of Geophysical Research: Atmospheres*, 118, 6905–6915. https://doi.org/10.1002/jgrd.50508
- Saunders, C. P. R., Keith, W. D., & Mitzeva, R. (1991). The effect of liquid water on thunderstorm charging. *Journal of Geophysical Research:* Atmospheres, 96(D6), 11007–11017. https://doi.org/10.1029/91jd00970
- Savtchenko, A., Mitzeva, R., Tsenova, B., & Kolev, S. (2009). Analysis of lightning activity in two thunderstorm systems producing sprites in France. *Journal of Atmospheric and Solar-Terrestrial Physics*, 71, 1277–1286. https://doi.org/10.1016/j.jastp.2009.04.010
- Sentman, D. D., Wescott, E. M., Osborne, D. L., Hampton, D. L., & Heavner, M. J. (1995). Preliminary results from the Sprites94 aircraft campaign: 1. Red sprites. *Geophysical Research Letters*, 22(10), 1205–1208. https://doi.org/10.1029/95gl00583
- Siemen, S., Russell, I., Quintino, T., & Varela Santoalla, D. (2016). Software updates in preparation for model cycle 41r2. ECMWF Newsletter
- Soula, S., van der Velde, O., Montanyà, J., Neubert, T., Chanrion, O., & Ganot, M. (2009). Analysis of thunderstorm and lightning activity associated with sprites observed during the EuroSprite campaigns: Two case studies. *Atmospheric Research*, 91(2–4), 514–528. https://doi.org/10.1016/j.atmosres.2008.06.017
- Stewart, S. R. (2016). Tropical cyclone report: Hurricane Matthew. National Hurricane Center.
- Takahashi, T. (1982). Electrification and precipitation mechanisms of maritime shallow warm clouds in the tropics. *Journal of the Meteorological Society of Japan*, 60, 508–519. https://doi.org/10.2151/jmsj1965.60.1_508
- Thomas, J. N., Solorzano, N. N., Cummer, S. A., & Holzworth, R. H. (2010). Polarity and energetics of inner core lightning in three intense North Atlantic hurricanes. *Journal of Geophysical Research: Atmosphere*, 115, A00E15. https://doi.org/10.1029/2009JA014777
- Warner, J. (1970). The microstructure of cumulus cloud. Part III. The nature of the updraft. *Journal of the Atmospheric Sciences*, 27, 682–688. https://doi.org/10.1175/1520-0469(1970)027<0682:tmoccp>2.0.co;2
- Williams, E., Downes, E., Boldi, R., Lyons, W., & Heckman, S. (2007). Polarity asymmetry of sprite-producing lightning: A paradox? *Radio Science*, 42, RS2S17. https://doi.org/10.1029/2006RS003488
- Yang, J., Qie, X., & Feng, G. (2013). Characteristics of one sprite-producing summer thunderstorm. Atmospheric Research, 127, 90–115. https://doi.org/10.1016/j.atmosres.2011.08.001
- Zhang, W., Zhang, Y., Zheng, D., & Zhou, X. (2012). Lightning distribution and eyewall outbreaks in tropical cyclones during landfall. Monthly Weather Review, 140, 3573–3586. https://doi.org/10.1175/mwr-d-11-00347.1
- Zheng, D., Zhang, Y., & Meng, Q. (2018). Properties of negative initial leaders and lightning flash size in a cluster of supercells. *Journal of Geophysical Research D: Atmospheres*, 123(22), 12857–12876. https://doi.org/10.1029/2018jd028824

HUANG ET AL. 15 of 15